Physics Faculty Research & Creative Works   Physics

Collisional Redistribution Of Polarized Radiation For Sr-ar(He) Systems: A Numerical Comparison Of The Semiclassical Decoupiing/locking Model To Exact Results

Ronald James Bieniek
Missouri University of Science and Technology, bieniek@mst.edu

Paul S. Julienne

Rank Rebentrost

Recommended Citation

R. J. Bieniek et al., "Collisional Redistribution Of Polarized Radiation For Sr-ar(He) Systems: A Numerical Comparison Of The Semiclassical Decoupiing/locking Model To Exact Results," *Journal of Physics B: Atomic, Molecular and Optical Physics*, vol. 24, no. 24, pp. 5103 - 5119, IOP Publishing, Dec 1991.
The definitive version is available at https://doi.org/10.1088/0953-4075/24/24/010

Collisional redistribution of polarized radiation for Sr-Ar(He) systems: a numerical comparison of the semiclassical decoupling/locking model to exact results

To cite this article: R J Bieniek *et al* 1991 *J. Phys. B: At. Mol. Opt. Phys.* **24** 5103

View the article online for updates and enhancements.

Collisional redistribution of polarized radiation for Sr–Ar(He) systems: a numerical comparison of the semiclassical decoupling/locking model to exact results

Ronald J Bieniek†, Paul S Julienne‡ and Frank Rebentrost§

† Department of Physics and Laboratory for Atomic and Molecular Research, University of Missouri-Rolla, Rolla, MO 64501-0249, USA
‡ National Institute of Standards and Technology, Gaithersburg, MD 20899, USA
§ Max-Planck-Institut für Quantenoptik, D8046 Garching, Federal Republic of Germany

Abstract. Semiclassical formulations of collisional redistribution of polarized radiation are presented at several levels of approximation, from full classical path coupled equations to the locking/decoupling model. These are numerically tested against the results of a quantum mechanical coupled-channels formalism, by the comparison of polarization curves in both spectral wings of the $Sr(^1S_0{-}^1P_1)$ transition, with Ar and He as collisional perturbers. It is found that the locking/decoupling model can often produce good agreement with exact results if the effects due to trajectories and multiple Condon points are treated properly. Significant discrepancies due to the Condon approximation used by the model are seen in the near blue wing of the spectra and attributed to antistatic effects. A clear analysis of these effects and the role of ambiguities introduced by the locking/decoupling radius is possible by a comparison with classical path methods in which the effects of radiative coupling and of rotational decoupling can be tested separately with a high degree of accuracy.

1. Introduction

When polarized radiation is absorbed during a collision or half-collision, the atomic fluorescence occurring after the fragments separate exhibits depolarization. This redistribution of polarized radiation can be used as a probe for long-range potentials, and the transition regime between atomic and molecular domains [1–5]. Although a quantum mechanical coupled-channels formalism has been developed to describe and numerically treat this redistribution process in atom–atom collisions [6, 7], investigators often use semiclassical models to explain and visualize the underlying causes of observed effects. One popular model is the locking/decoupling model suggested by Lewis *et al* [8]. In this picture, the depolarization is due to the rotation of excited orbitals which are locked for a time to the internuclear axis, but then suddenly remain space-fixed at some decoupling radius [8, 9]. In earlier work by Cooper the validity of this model was discussed and compared for the Sr–Ar case with several numerical methods using straight-line paths [10]. Even with a crude mimicking of true trajectories by two straight-line segments, it has been shown that curved trajectories have a significant effect on the polarization in this model [11]. It is clear that accurate classical paths are needed in general for a successful modelling of depolarization data in

optical collisions, as was found in alkali rare-gas systems [12]. Yet, even with accurate classical-path trajectories, it has not been clear how accurately semiclassical models can predict redistribution. The purpose of this paper is to explore this issue.

We present, in the following, the detailed equations required to compute polarization curves from accurate trajectories within the locking/decoupling model. After that, we set down the full classical path, radiatively coupled equations that describe redistribution, and discuss the approximations that lead from them to the locking/decoupling model of orbital rotation. This includes an 'exact' way of determining the decoupling radius in the context of the model's assumptions. Numerical polarization curves are displayed and discussed for the red and blue spectral wings of the $Sr(^1S_0-^1P_0)$ transition, for both Ar and He collision partners at several energies. The numerical results for various levels of semiclassical approximation and for different choices of decoupling criteria are compared with the results obtained from 'exact' quantum computations.

2. The semiclassical locking/decoupling radius model

The main improvement in the present semiclassical model is that true trajectories were used to compute the rotation angle of the excited electronic orbital. Under the locking/decoupling radius model, this is the same angle through which the internuclear axis rotates from the excitation point to the decoupling point, where it is assumed there is a sudden transition from molecular to atomic domains. In this view, the colliding atoms initially travel along the ground molecular state potential, and then suddenly find themselves on an excited molecular state potential if they absorb a photon at one of the allowed Condon points (R_c), where a vertical transition may occur. These points $R_c(\delta)$, which depend upon detuning δ from the line centre, satisfy $\Delta V_s(R_c) - \Delta V_s(\infty) = hc\delta$, where $\Delta V_s(R) = V_s(R) - V_i(R)$ is the potential difference between the ground state i and the excited s state. The electronic orbital then rotates with the internuclear axis as the collision continues on the excited potential, until the colliders are separated by some decoupling radius R_{dc}. The excited orbital then suddenly ceases to rotate with the internuclear axis, and maintains its space-fixed orientation throughout the remainder of the collision, until the Sr atom fluoresces at the 460.7 nm line $(^1S_0-^1P_1)$. As far as the colliders are concerned, they are merely travelling along one continuous surface, which is comprised of the ground- and excited-state potentials cut and patched together along the transitional cut.

Since the excited surface is spherically symmetric, we can use well known formulae for the central potentials to compute the rotation angle $\Omega_s(b_f, R_x)$ which depends upon the equivalent impact parameter b_f of the final state, the initial rotation radius $R_x = \min(R_c, R_{dc})$, the excited potential surface s, and the decoupling radius R_{dc}. It also depends upon whether excitation occurs on the incoming or outgoing part of the trajectory. The rotation angles for incoming (Ω_s^i) and outgoing (Ω_s^o) rotation angles on excited molecular state s are given by

$$\Omega_s^i(b_f, R_x) = 2\theta_s(b_f, R_t^s) - \theta_s(b_f, R_x^s) - \theta_s(b_f, R_{dc})$$
$$\Omega_s^o(b_f, R_x) = \theta_s(b_f, R_x^s) - \theta_s(b_f, R_{dc})$$

(1)

where

$$\theta_s(b, R) = -\frac{\pi}{2} + bv_s \int_R^\infty \frac{dr}{r^2 v_s(b, r)}$$

(2)

$R_t^s(b)$ is the turning point for the collision, while $v_s(b, r)$ is the radial velocity for impact parameter b and radius r on molecular potential s, v_s being the asymptotic limit $v_s(b, r \to \infty)$. The impact paramenter b_f of the final state is related to that of the initial state by the angular momentum conserving relationship $(E + hc\delta)b_f^2 = Eb^2$, where E is the initial collisional energy.

Let $k_\Sigma(\delta)$ be the absorption coefficient from the initial molecular state to an excited Σ state, and let $k_\Pi(\delta)$ be the absorption coefficient to a doubly degenerate excited Π state with the same asymptote as the Σ state. We now assume that no interference occurs among transition points of the same detuning, and that the quasistatic approximation gives the relative weighting of transitional probabilities at the Condon points R_c. Some support for this is obtained from ancillary close-coupled quantal computations that demonstrated that Σ–Π interference had little effect on the $k_{\Sigma,\Pi}$ coefficients; values obtained with and without Σ–Π coupling included in the calculations only differed by a few per cent. However, this is only true after summing the partial-wave contributions by which a great deal of randomizing cancellations occurred in the interference terms. Interference among transitions between the same potentials can have significant effects (e.g. the Σ satellite structure in the red wing), and is a drawback of the utilitarian quasistatic theory description used here. Yet, within this approximation, the Stokes parameter $P(\delta)$ for the degree of post-collision linear polarization is then given by [8, 13]

$$P(\delta) = \frac{3\alpha^{(2)}(\delta)}{2 + \alpha^{(2)}(\delta)} \tag{3}$$

where, setting $f(\delta) = 2k_\Sigma/k_\Pi$,

$$\alpha^{(2)} = \frac{[\frac{1}{6} + \frac{1}{5}\langle\cos(\Omega_\Pi)\rangle + \frac{1}{10}\langle\cos(2\Omega_\Pi)\rangle] + f(\delta)[\frac{1}{30} + \frac{1}{10}\langle\cos(2\Omega_\Sigma)\rangle]}{\frac{2}{3} + \frac{1}{3}f(\delta)}. \tag{4}$$

By quasistatic theory (which assumes no coherence between transition events) the excitation rates are

$$k_s(b) \sim \sum_c \frac{(\mu_c^s)^2}{\Delta V_s'(R_c^s)v_s(b, R_c^s)} \qquad b < b_{\max}$$

$$k_s^{\mathrm{tot}} = 2\pi \int k_s(b)b\,\mathrm{d}b \sim \sum_c \frac{(\mu_c^s)^2(R_c^s)^2(1 - V_c^s/E)^{1/2}}{\Delta V_s'(R_c^s)} \tag{5}$$

where $b_{\max} = R_c^s[1 - V_c^s/E]^{1/2}$, $V_c^s = V_s(R_c^s)$ and $\mu_c^s = \mu_s(R_c^s)$, is the transitional dipole moment. The angle average in (4) then becomes

$$\langle\cos(q\Omega_s)\rangle = \frac{1}{2}\int_0^\infty \frac{k_s(b)}{k_s^{\mathrm{tot}}}\{\cos[q\Omega_s^o(b_f, R_x^s)] + \cos[q\Omega_s^i(b_f, R_x^s)]\}2\pi b\,\mathrm{d}b$$

$$= \sum_c \frac{(\mu_c^s)^2/|\Delta V_s'(R_c^s)|}{\sum_n(R_n^s\mu_n^s)^2(1 - V_n^s/E)^{1/2}/|\Delta V_s'(R_n^s)|}$$

$$\times \frac{1}{2}\int_0^{b_{\max}}\{\cos[q\Omega_s^o(b_f, R_c^s)] + \cos[q\Omega_s^i(b_f, R_c^s)]\}b\,\mathrm{d}b/v_s(b, R_c^s). \tag{6}$$

With a change of the integration variable in which b is replaced by a scaled radial velocity at R_c^s,

$$x = \frac{v_s(b, R_c^s)}{v_s} = \left[1 - \left(\frac{b}{b_{max}}\right)^2\right]^{1/2} \tag{7}$$

the averages of the rotational angles have the form

$$\langle\cos(q\Omega_s)\rangle = \sum_c \frac{(R_c^s \mu_c^s)^2 (1 - V_c^s/E)^{1/2}/|\Delta V_s'(R_c^s)|}{\sum_n (R_n^s \mu_n^s)^2 (1 - V_n^s/E)^{1/2}/|\Delta V_s'(R_n^s)|}$$
$$\times \frac{1}{2}\int_0^1 \{\cos[q\Omega_s^i(b_f, R_c^s)] + \cos[q\Omega_s^o(b_f, R_c^s)]\}\,\mathrm{d}x \tag{8}$$

with

$$b_f = \left(\frac{E}{E + hc\delta}\right)^{1/2}\sqrt{1 - x^2}\,b_{max}. \tag{9}$$

Because the quasistatic approximation has been used to estimate the relative contribution of individual impact parameters, interference effects are not incorporated into the weighting of rotational angles. However, the factors in front of the integrals should distribute the total absorption strength amongst multiple contributing Condon points in a reasonably accurate way, no matter what the source of the absorption coefficients $k_s(\delta)$ employed to determine the ratio $g(\delta)$.

The only freedom one has in the locking/decoupling radius model described here is the method by which the decoupling radius R_{dc} is chosen. Various methods have been suggested in the literature. Three different methods are reported here, hereafter referred to as M1, M2 and M3. The first two employ an adjustable constant β, which is expected to be near unity. The methods are given in the following.

2.1. M1

The accumulated phase difference between excited states is within a critical value β_1 of their asymptotic difference

$$\left|\int_{R_{dc}}^\infty \frac{\Delta V^*(r)\,\mathrm{d}r}{\hbar v_f}\right| = \beta_1 \tag{10}$$

where $\Delta V^*(r)$ is the potential difference between the excited states, and v_f is the asymptotic velocity in the final state (see [1]).

2.2. M2

An energy–uncertainty relationship suggested by Lewis *et al* [8]

$$|\Delta V^*(R_{dc})|\frac{b_f}{\hbar v_f} = \beta_2. \tag{11}$$

A similar criterion for the decoupling radius was derived by Grosser [14], with b_f replaced by R_{dc} in (11). Additional computations showed that it produces results very similar to the Lewis definition (but with different optimal values of β). In general, as β in methods M1 and M2 is decreased, the decoupling radius R_{dc} increases. This produces a decrease in polarization, because the rotation angle Ω is larger.

2.3. *M3*

An 'exact' definition of the decoupling radius [15, 16] is obtained by solving the coupled semiclassical equations for the time evolution of the electronic states along a classical path. The rotation of the excited molecular orbital is then accurately computed from its alignment angle up to asymptotic separation. With this a unique R_{dc} can be determined that reproduces this rotation angle in a classical trajectory under the assumption that the orbital rigidly follows the rotation of the intermolecular axis up to this point from whereon it remains space-fixed. This procedure has been described for the case of full collisions by Hertel *et al* [1] and was used in the present context to examine the concepts underlying the locking/decoupling model [16]. There is no adjustable parameter β in this method. It should, however, be noted that the decoupling radius determined by M3 is just an artifact extracted to make the connection with the locking/decoupling model. The solution of the coupled semiclassical equations is inherently superior to this model, since the locking radius model can be seen as an approximation to it.

3. The foundation of the locking/decoupling model in the framework of classical path theory of optical collisions

The locking/decoupling model introduced previously rests on a number of approximations, of particular importance being: (a) the classical description, which uses a particular choice of trajectories switching at the Condon points of the optical transitions, and (b) the sudden decoupling of angular momentum in the transition from the molecular to the atomic coupling cases. These assumptions, however, need to be discussed from a broader viewpoint.

The classical trajectory approach employed is most naturally seen in the context of a full semiclassical description, e.g. by classical-limit quantum mechanics [17]. Such an approach requires one to find specific trajectories for a given transition and the coherent superposition of all resulting amplitudes. When applied to electronically inelastic collisions, the theory essentially reduces to a classical description in regions where the couplings between the adiabatic states can be ignored. In regions where non-adiabatic couplings are critical, one could follow the trajectories to the complex intersection points of the adiabatic potentials to obtain the transition probabilities. For the problem considered here, there are thus two crucial regions in the model. The first is at the Condon points, which are the points of avoided crossing between the dressed molecular states. In this case, we will not use complex trajectories, and instead use real trajectories that switch from the ground to the excited state at exactly the Condon points. Studies of the validity of the classical path method (see e.g. [18]) show that often a trajectory propagated under the action of a mean force $F = (F_1 F_2)^{1/2}$ is the optimal choice for the calculation of transition probabilities. Another choice used in the context of calculations of excitation spectra is formed by the mean force $F = \frac{1}{2}(F_1 + F_2)$ [19]. The advantage of the present curve-switching trajectories is that they also form a realistic description in regions far from the Condon points. They should, however, also give reliable results in the excitation region as long as the turning point is not close to the Condon point or the latter is classically inaccessible. The second region is where the uncoupling of angular momentum from the internuclear axis occurs in the upper manifold. Here, however,

the detailed nature of the trajectory may not be so critical because the potentials are usually small in such long-range regions and have little effect on the trajectory.

Furthermore, the concept of a decoupling radius makes use of a number of implicit assumptions that are not valid in general. (a) The transition from the molecular to the atomic coupling case is described as a rotation of the orbital prepared by the optical transition. An important problem connected with this assumption is that, due to the typical curve crossing of the excited Σ and Π terms, considerable additional mixing among these states may occur. This is then reflected in a change of the orbital shape; (b) the decoupling region must be sufficiently localized; (c) an *a priori* criterion similar to the ones mentioned earlier must be available to determine this region. Among the problems connected with (b) and (c) is that such a generally applicable criterion does not exist. Approximate estimates are, however, ambiguous in the sense that they can only be qualitative, particularly when applied to typical systems involving neutrals, where the asymptotic degeneracy is not lifted rapidly enough under thermal collisions. In addition the criteria often have no unique solution for the typical non-monotonic potential difference between excited states; and (d) although spin is not relevant for a system like Sr–Ar, it is quite obvious that the concept of a localized decoupling must be questioned more carefully if other small interactions such as spin–orbit coupling intervene in the decoupling region, as in the study of alignment effects in alkali–rare-gas collisions [20, 21].

In the following we will discuss the results of the decoupling model on the basis of more general classical path approaches, in which the approximations made in the model can be systematically investigated without giving up its classical content. In the framework of classical path theory an optical collision in a system like Sr–Ar is described by a set of four coupled equations

$$i\hbar \dot{c}_i = \sum_j [H_{ij}'^{\text{el}} + H_{ij}'^{\text{rad}}] c_j \tag{12}$$

for the non-degenerate ground state ($i = 1$) and the triply-degenerate excited state ($i = 2, 3, 4$ for the three components $m = -1, 0, 1$) of the Sr atom. These equations were used by Light and Szöke [23] to study the effect of strong fields on Sr + Ar collisions. They chose the space-fixed (primed) frame for the electronic and radiative Hamiltonians to which the scattering boundary conditions and the optical field are naturally referenced. These electronic and radiative Hamiltonians are related to those in a body-fixed (unprimed) frame by a transformation

$$H' = \mathcal{R}(\phi, \theta, 0) H \mathcal{R}^\dagger(\phi, \theta, 0). \tag{13}$$

Here the rotation operator $\mathcal{R}$ involves the instantaneous angles of the internuclear axis θ, ϕ. The body-fixed matrix H^{el} is diagonal with the potential terms. The radiative coupling (in the dipole approximation) connects the ground level with the excited levels. As the rotating wave approximation for the radiative interaction is used, its explicit time dependence is removed by using molecule + radiation field

states instead of the states i. Then

$$H^{\rm el} = \begin{pmatrix} \Sigma_g + \hbar\omega & 0 & 0 & 0 \\ 0 & \Pi & 0 & 0 \\ 0 & 0 & \Sigma & 0 \\ 0 & 0 & 0 & \Pi \end{pmatrix}$$

$$H^{\rm rad} = \begin{pmatrix} 0 & \mu_\Pi E_1 & \mu_\Sigma E_0 & \mu_\Pi E_{-1} \\ \mu_\Pi E_1^* & 0 & 0 & 0 \\ \mu_\Sigma E_0^* & 0 & 0 & 0 \\ \mu_\Pi E_{-1}^* & 0 & 0 & 0 \end{pmatrix}.$$

(14)

In the molecular frame the electronic Hamiltonian is thus readily obtained from the potentials of the ground and excited states. The radiative interaction involves the instantaneous projections of the space-fixed field E and the transition dipoles for the two transitions. Equivalently, the classical path equations can be written in a body-fixed frame, in which the rotational coupling among the electronic states in the upper manifold is apparent. This approach will be followed here.

The collision system itself has symmetry with respect to reflection by the collision plane, as long as we can ignore the small contribution of the electronic angular momentum to the total angular momentum. This is because, in the rotational coupling operator [24]

$$- i\hbar\langle j|(\partial/\partial t)|i\rangle = -\dot\theta\langle j|L_y|i\rangle + \dot\phi[-\langle j|L_z|i\rangle\cos\theta + \langle j|L_x|i\rangle\sin\theta] \tag{15}$$

only the first term on the right-hand side is important. Equation (15) represents the Coriolis interaction

$$H^{\rm cor} = -\frac{JL}{mR^2} \tag{16}$$

where J and L are the total and electronic angular momenta, respectively. With the choice of the collision plane as the xz plane the only significant contribution to J is from the rotational angular momentum of the nuclei $l = r \times p$ which has no x and z components. As a consequence the rotational coupling affects only the in-plane component.

The $+/-$ symmetry is of no advantage for an arbitrarily oriented very strong optical field. However, if the optical field is not too strong (as is the case here), we can treat its components parallel and perpendicular to the collision plane separately. The coupled-path equations then reduce to two independent sets of equations for the two symmetry cases

$$i\hbar\dot c_\Sigma^+ = \tfrac{1}{2}\mu_\Sigma E^+ \cos\theta \exp\left\{i\omega t + \hbar^{-1}\int^t {\rm d}\tau[V_g(\tau) - V_\Sigma(\tau)]\right\} c_g$$

$$+ \dot\theta\langle\Sigma|L_y|\Pi^+\rangle \exp\left\{i\hbar^{-1}\int^t {\rm d}\tau[V_\Sigma(\tau) - V_\Pi(\tau)]\right\} c_\Pi^+$$

$$i\hbar\dot c_\Pi^+ = \tfrac{1}{2}\mu_\Pi E^+ \sin\theta \exp\left\{i\omega t + \hbar^{-1}\int^t {\rm d}\tau[V_g(\tau) - V_\Pi(\tau)]\right\} c_g$$

$$+ \dot\theta\langle\Pi^+|L_y|\Sigma\rangle \exp\left\{-i\hbar^{-1}\int^t {\rm d}\tau[V_\Sigma(\tau) - V_\Pi(\tau)]\right\} c_\Sigma^+$$

(17)

and

$$i\hbar\dot{c}_\Pi^- = \tfrac{1}{2}\mu_\Pi E^- \exp\left\{i\omega t + \hbar^{-1}\int^t d\tau[V_g(\tau) - V_\Pi(\tau)]\right\}c_g. \tag{18}$$

In this limit of weak fields, the ground state changes little, and $c_g(t) = 1$ for all times. Here and in the following, the time dependence in the potentials enters through the trajectory. Thus $V(\tau)$ is used instead of $V[R(\tau)]$. A further simplification occurs by noting that often the asymptotic (large R) value of the matrix element of L_y, i.e. $\langle\Pi^+|L_y|\Sigma\rangle = i$, may be used to a good approximation.

These classical path equations with full radiative coupling between ground and excited states (referred in the following as the CPR equations) are solved here using the canonical trajectories that switch between these states at the Condon points. As discussed before, this is consistent with semiclassical theory. It is to be noted that using an averaged potential

$$V_{ave} = \sum_i c_i^* c_i V_i \tag{19}$$

to determine the trajectory leads to unacceptable results, since this average potential is then, effectively, the ground-state potential. Like any method employing strictly classical trajectories, the actual implementation of the CPR equations is still somewhat ambiguous in the presence of multiple transition locations. For the near-red wing in the Sr–Ar system, there are three transition points $R_c(\delta)$, one for Π and two for Σ excitation. Each R_c is further traversed on the incoming and outgoing motions of the system. Thus six different trajectories and rotation angles would result from switching at the different locations, and the phased contributions from all possible transition events would have to be properly combined. In this paper, we will, however, apply the CPR equations numerically only in the fairly clear-cut situation of the blue wing, where a single R_c for Σ excitation exists. Another point is the contribution from trajectories with impact parameters $b > b_{max}$ for which the Condon point is no longer reached classically. A crude treatment of this region was performed by choosing the trajectories to switch potential at the outer of the two turning points of the radial motion. It proved sufficient for the present purpose to estimate the non-classical contribution and to demonstrate convergence of the results. Note that this choice smoothly connects at b_{max} with the curve-switching trajectories introduced earlier for $b < b_{max}$.

Since the optical field is present in the asymptotic region, a proper initial condition for the CPR equations is $c_I = 1$, with I denoting the dressed ground-state-like eigenstate of the separated atoms plus radiation field Hamiltonians. Likewise the transition amplitudes are defined for transitions between dressed states. It was shown in [25] that these amplitudes reduce to the usual weak-field distorted wave description for $\hbar\delta \gg \mu E$. Equations (17) and (18) are equally valid in the impact regime and in the far wings. Given the solutions of the CPR equations for the three specific directions of the field along the coordinate axes of the collision frame, the $\alpha^{(2)}$ can be determined directly from the corresponding multipoles, i.e. without reference to a rotation angle. The procedure involves the rotation applied to field and the final atomic states between the collision and space-fixed frames and the averaging over the isotropic distributions of collision planes. With this respect it is completely analogous to the case of the rotation model [8, 12]. The impact parameter averaging for the

CPR method proceeds however as usual, i.e. without the inverse velocity factor v_s^{-1} in (6) that accounts for the transit time through the Condon region in the rotation model.

If one formally integrates the CPR equations, one notices that the transition from the ground state to the excited state predominantly occurs around the stationary-phase points

$$hc\delta = V_e(R_c) - V_g(R_c) \qquad (20)$$

where R_c are the Condon points for a vertical transition. For regions distant from the Condon points, the radiative coupling term in (17) and (18) will have no cumulative influence. The coupled equations thus reduce to a second and more approximate form, when the radiative coupling is treated within the Condon approximation. In this approximation the optical transition occurs in a region around a definite Condon point and can be ignored from then on, and only the rotational mixing of the upper two terms still needs to be considered. This leads to the equations

$$i\hbar\dot{c}_\Sigma^+ = \dot{\theta}\langle\Sigma|L_y|\Pi^+\rangle \exp\left\{i\hbar^{-1}\int^t d\tau\,[V_\Sigma(\tau) - V_\Pi(\tau)]\right\} c_\Pi^+ \qquad (21)$$

$$i\hbar\dot{c}_\Pi^+ = \dot{\theta}\langle\Pi^+|L_y|\Sigma\rangle \exp\left\{-i\hbar^{-1}\int^t d\tau\,[V_\Sigma(\tau) - V_\Pi(\tau)]\right\} c_\Sigma^+ \qquad (22)$$

which are solved for an initial condition in which only the component to which the Condon transition leads is non-vanishing. These classical path equations in the Condon approximation will be labelled CPC. The time dependence appearing in (21) is solely determined by a trajectory in the upper state. As long as only a single Condon point is involved, the transition probability from the ground to the excited state plays no role in calculating the polarization. Similar to the treatment of the locking/decoupling radius model in section 2, one can use some supplemental method of weighting probabilities, e.g. quasistatic theory, in the case of multiple Condon points. The use of switched potentials for the calculation of numerical trajectories is the obvious choice for the CPC method. Any reasonable averaging over the two excited states would produce only a marginal effect, since the potential in the region where strong rotational coupling occurs is typically of the order of 10 cm^{-1}, and the trajectory is then no longer affected by it. The calculations reported here were thus performed with trajectories propagated at all later times on the excited state reached by the Condon transition.

Some characteristic problems of the Condon approximation are apparent, e.g. when dealing with multiple stationary phase points and interferences between them. Even if there is only a single Condon point, the interference of amplitudes resulting from the two canonical trajectories must be considered. Its effect is, however, expected to be of little importance, as the deflection functions of both trajectories are usually quite different. As in the classical decoupling model, only the motion after excitation will affect the results.

This approach therefore forms the background for the more simplistic description underlying the rotational model for depolarization. Since the rotational decoupling of electronic angular momentum from the axis is likely to be described accurately by the CPC approach, it does not rely on the concept of a decoupling radius. Furthermore,

solving the CPC equations provides insight into the full motion of the orbital after excitation. In particular the rotation of the orbtital up to the final dissociation of the collision pair can be monitored directly by the 'alignment' angle γ of the orbital [1]

$$\tan 2\gamma = \frac{2\operatorname{Re}\{a_\Sigma^+ a_\Pi^{+*}\}}{|a_\Sigma^+|^2 - |a_\Pi^+|^2} \qquad (23)$$

where

$$a_{\Sigma,\Pi} = c_{\Sigma,\Pi} \exp\left\{-\mathrm{i}\hbar \int^t \mathrm{d}\tau\, V_{\Sigma,\Pi}(\tau)\right\}. \qquad (24)$$

The angle γ defined by (23) is exactly the angle that is needed in a rotation model for depolarization; one may therefore circumvent the introduction of the decoupling radius. It is only for the purpose of making a connection with the classical model that we define an equivalent decoupling radius by the scheme shown in figure 1. R_{dc} is chosen to be at the intersection of the curves describing asymptotic body-fixed and space-fixed behaviours. This expresses the condition that the rotation angle between excitation and decoupling is exactly equal to the rotation angle of the orbital between excitation and infinity [15]

$$\Omega = \theta(R_{\mathrm{dc}}) - \theta(R_{\mathrm{c}}) = \gamma(\infty) - \gamma(R_{\mathrm{c}}). \qquad (25)$$

This equation is thus the defining equation for the 'exact' decoupling radius R_{dc}. Method M3 uses the properties of the CPC solutions to determine this value, and may thus be seen as the most accurate representation of the locking/decoupling model.
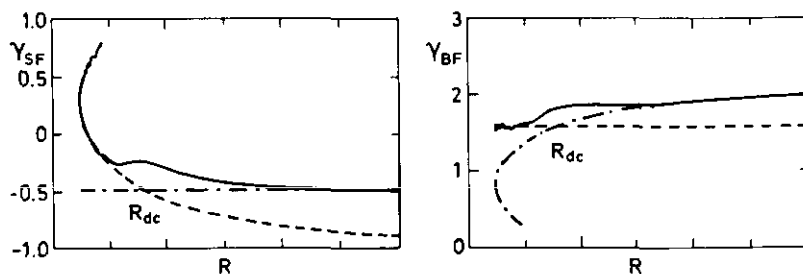

Figure 1. Determination of an effective, semiclassically 'exact' decoupling radius from the classical path solutions of the rotational coupling problem (method M3). The curves show the rotation of the orbital after excitation (full curve) and of the molecular axis (broken curve), seen in either a space-fixed (SF) or a body-fixed (BF) frame attached to the molecule. The decoupling radius R_{dc} is defined by the intersection of the dependencies for rigid rotation of the orbital with the axis (broken curve) and of complete decoupling in the asymptotic region (chain curve). For details see section 3.

An understanding of the behaviour of the polarization seen in the near blue wing of the Sr–Ar system is obtained only after examining the role of the two main features involved in the decoupling model calculations, i.e. the Condon approximation and the choice of the decoupling radius. It will be shown later that none of the various suggested methods to determine a decoupling radius lead to a reasonable reproduction of all the features seen in the spectra. An accurate analysis is, however, possible by using the more sophisticated CPR classical path description.

4. Numerical results

For Sr–rare-gas collisions, there is a ground $X\Sigma$ potential, and two relevant excited potentials, $A\Pi$ and $B\Sigma$. The numerical potentials employed here were the same ones used in the quantum computations by Julienne and Mies for the Sr–Ar system [6]. To test the rotational aspects of the semiclassical model, exact absorption coefficients from the quantum calculations were used to compute the ratio $g(\delta)$ for the relative strength of the transitions to the two different excited states. Although the quantum coupled-channels method does not formally consider the $A\Pi$ and $B\Sigma$ contributions separately, but rather as coupled, an effective $k_\Pi(\delta)$ can be accurately obtained as twice the Q-branch absorption coefficient. The contribution of absorption to the $B\Sigma$ state is just the quantum total absorption coefficient minus twice the Q-branch. These approximations were confirmed by computing the coefficients directly using quantal distorted-wave methods on the $A\Pi$ and $B\Sigma$ potentials [11]; the results agreed to within 1%.

Sometimes there arise situations in which there are multiple values of the decoupling radius that satisfy the criterion of M1 or M2. In such cases, the outermost one has been selected for R_{dc}. Furthermore, there are occasions on which the excitation radius is outside the decoupling radius. Under these circumstances, it has been assumed that rotation begins when the excited-state trajectory reaches R_{dc} (implying the rotation angle is zero for an outgoing excitation) [11].
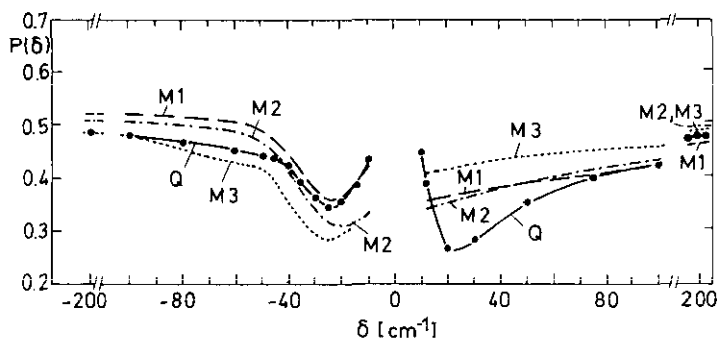

Figure 2. Redistributed polarization P (Stokes parameter) as a function of detuning δ for Sr–Ar at a collisional energy of $E = 500$ cm^{-1}. The dots are exact quantum mechanical values, labelled Q. The labels M1, M2, M3 refer to the method used to determine the decoupling radius. The line M1 is for method 1, with $\beta_1 = 0.75$; M2 refers to method 2, with $\beta_2 = 1.5$. The line M3 is generated by method 3 which has no β parameter.

Figure 2 displays the polarization for Sr+Ar collisions for an incident heavy-particle collisional energy of $E = 500$ cm^{-1}. The quantum results can be considered exact, and are the references against which the various semiclassical results can be tested. Semiclassical polarization curves for the three methods of determining the decoupling radius, with various values of β_1 and β_2, were computed and compared with the quantum results. (Subscripts on β and $P(\delta)$ refer to the method employed to determine the decoupling radius.) Values of β of the order of unity (0.5–1.5) did, indeed, generate curves that are in good qualitative agreement with exact results—except for small detunings in the blue wing ($\delta > 0$). (This discrepancy will be

discussed later.) Although there is a range of values of β for M1 and M2 that are generally equally good, they fall within a width of only 0.5 for a given method. Increasing β increases the polarization (by pushing the decoupling radius to smaller values), while producing only minor changes in the shape of the polarization curves. The best overall results were obtained with $\beta_1 = 0.75$ for method M1 and $\beta_2 = 1.5$ for M2 and these values were used in the graphical presentation of the results. Remarkably, however, method M3 for determining R_{dc} does not fare as well. This is surprising and bothersome, for it corresponds to an exact definition of the decoupling radius within the Condon approximation, without adjustable parameters (see (25)). This indicates that there is an inherent deficiency in the Condon approximation used by the decoupling-radius model.

Semiclassical theories should be at their best at larger detunings, since these are definitely out of the impact regime and arise from transitions to single potentials at a single Condon point. For Sr-rare gas, these are $X\Sigma-A\Pi$ transitions beyond the $X\Sigma-B\Sigma$ satellite in the red wing, and $X\Sigma-B\Sigma$ in the blue wing. Because the $X\Sigma-B\Sigma$ difference potential has an minimum, it gives rise to a classical red-wing satellite for detunings between about -40 and -10 cm^{-1}. (Note that in this detuning interval, there are three Condon points for each δ, one associated with the $A\Pi$ state, and two for the $B\Sigma$ state.) To obtain reasonable agreement in this detuning interval, we must choose $\beta_1 = 0.5$–0.75, even though the polarization P_1 (-200 cm^{-1}) is now too large. (Values of $\beta_1 \simeq 0.4$ achieved agreement at $\delta = -200$ cm^{-1}, but produced polarizations that were much too low for detunings near -30 cm^{-1}.) It is not surprising to see that all three decoupling-radius methods do well in predicting the polarization in the far-blue wing at $\delta = +200$ cm^{-1}, a region characterized by only a single Condon point $R_c(\delta)$ for $X\Sigma-B^2\Sigma^+$ transitions. This agreement is due to the fact that the excited state Σ potential is essentially repulsive and tends to backscatter the particles into the direction from which they came. Thus the rotation angle entering the model remains at small values. It should be noted that the Stokes parameter in this region is not far from the zero-rotation-angle limit of 0.5 ($a^{(2)} = 0.4$, see (4)).
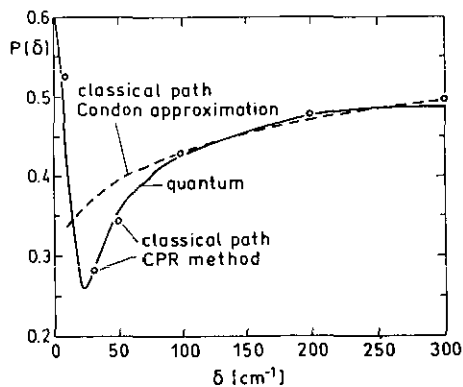

Figure 3. Stokes parameter for the polarization as calculated with the quantum coupled-channels method and by the classical path methods with the Condon approximation (CPC) and without it (CPR). For the latter cases, the trajectory was chosen to be on the upper Σ state.

In figure 3 we show in more detail that both the decoupling-radius model and the CPC calculations completely miss the dip in polarization around the detuning

$\delta \simeq +20$ cm^{-1}. The CPR approach, however, reproduces this feature, implying that the fault does not lie in the semiclassical approach, but rather in the Condon approximation. Since the quantal polarization rises at $\delta = 0$, one may expect that polarization *increases* as adiabatic approximations break down as one enters the impact regime, which would not explain the large *decrease* at $\delta = +20$ cm^{-1}. To give a plausible explanation of the dip, we note that $k_{\Pi}/k_{\Sigma} = 0.56$ at $\delta = 20$ cm^{-1}, implying antistatic (i.e. non-vertical, non-Condon) transitions to the AΠ state are significant. In the Condon approximation, no transitions to this state should occur, in contradiction to the actual situation. Absorption to the Π state even dominates for $\delta = 5$–15 cm^{-1}. Since AΠ transitions in the red wing produce a downward trend in polarization toward line centre, one may expect that the AΠ antistatic contribution would have a similar effect in the blue wing, causing the polarization to decrease more just before it rises in the line core. Since antistatic effects should decrease with decreasing collisional energy [26], polarizations were recomputed at $E = 200$ cm^{-1}. For this energy, the ratio of absorption coefficients has reduced to $k_{\Pi}/k_{\Sigma} = 0.14$ at $\delta = +20$ cm^{-1}. When compared with the value of 0.56 for $E = 500$ cm^{-1}, one sees that the AΠ absorption has indeed decreased. The blue-wing polarization curves for the lower collisional energy are displayed in figure 4, showing the improvement in the Condon approximation results and lending evidence to the explanation of the dip as a competition between antistatic and impact-regime effects.
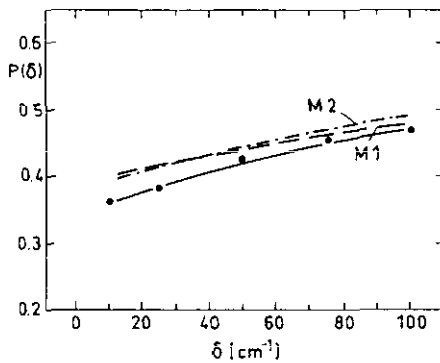

Figure 4 Blue wing of Sr–Ar at a collisional energy of $E = 200$ cm^{-1}. The labels are the same as those in figure 2.

The polarizations $P(\delta)$ for several detunings were computed at collisional energies E ranging between 200 and 2000 cm^{-1} to ascertain the general ability of the decoupling radius model to track the energy dependence. The quantum and semiclassical results are compared in figure 5. The range of β_1 that produced good tracking narrowed, the optimal β being $0.75 \sim \pi/4$. However, it was less good for P $(+200$ cm$^{-1})$ at a collisional energy of $E = 2000$ cm^{-1}, due to the fact that the phase integral of MI has a hump at large R of height 0.744 at this energy for $\delta = +200$ cm^{-1}. As one adjusts β_1 about this value, the decoupling radius suddenly jumps, increasing P from 0.402 to 0.465. This does reveal the problem of the ambiguity of multi-valued situations alluded to earlier. This, coupled with the sensitivity of $P(\delta)$ to changes in β_1, indicates that refinements in determining the decoupling radius, even within the structure of the present methods, may yield significant improvement. But even in its present form, the model does predict the correct energy
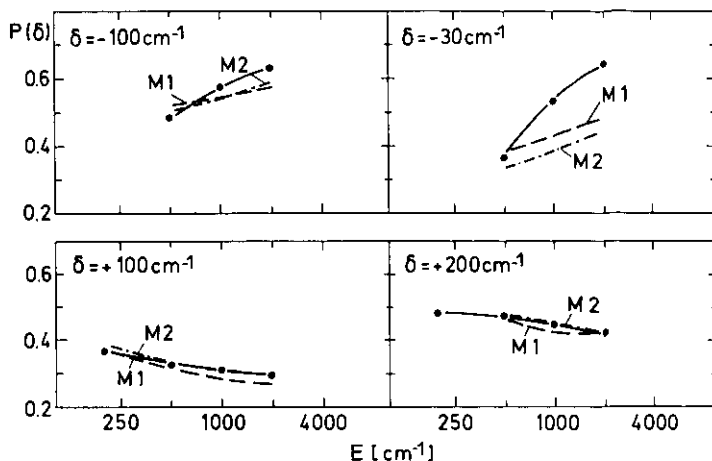
Figure 5. The collisional energy dependence of redistributed polarization in the Sr–Ar system. The labels are the same as those in figure 2.

trends; polarization increases with energy in the red wing, and decreases in the far blue.

To investigate the mass dependence of polarization and the ability of the decoupling radius model to handle it, quantum and semiclassical computations were conducted on the Sr–He system, changing only the reduced mass to the appropriate value, while retaining the same intermolecular potentials as the Sr–Ar system. In this way, the collisional reduced mass is the only changed parameter in the calculation. Although the Condon points for transitions and the potential surfaces do not change, the absorption coefficients, trajectories and decoupling radii are affected. The full polarization curves for Sr–He at a collisional energy of $E = 500$ cm^{-1} are shown in figure 6. The exact and decoupling-radius results exhibit increased polarization in comparison to the Sr–Ar system.
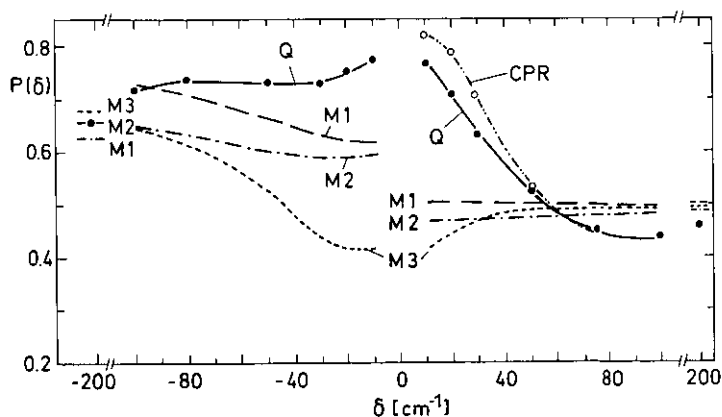

Figure 6. Redistributed polarization for Sr–He at a collisional energy of $E = 500$ cm^{-1}. The labels are the same as those in figure 2. Also shown are results obtained with the CPR method.

The exact and all semiclassical results exhibit increased polarization in comparison

with the Sr–Ar system. But it is obvious that the general agreement is less good between quantal and semiclassical results in the Sr–He system than in Sr–Ar. One might attribute the mid-wing discrepancies to the extension of the impact regime to larger detunings. Yet the good results obtained from the CPR equations undermine this inference. Since quantal distorted-wave techniques, when properly implemented, can obtain correct results in the impact limit [25], one expects that the semiclassical methods described here could behave well nearer to line centre if enhanced to mimic phased contributions from different transitional paths. The CPR approach does well in the mid-blue-wing interval because it approximately handles the relationships between Condon Σ transitions and antistatic Π contributions. The antistatic effects are considerable larger for the lighter target; $k_\Pi/k_\Sigma = 1.95$ at $\delta = +20$ cm^{-1}, implying antistatic absorption actually dominates there, in comparison with its lower (yet significant) role in Sr–Ar where $k_\Pi/k_\Sigma = 0.56$. The increased antistatic effect for smaller reduced mass muddles the behaviour of polarization in the boundary region between quasistatic and impact domains, and is a significant problem to be addressed in future work on semiclassical descriptions of redistribution. The disagreements between the locking/decoupling radius model and the quantum results for P ($+200$ cm^{-1}) is bothersome, since this should be beyond the impact regime and into the static. Furthermore, the tracking of polarization with incident energy E is less good, as shown in figure 7. The cause of this is unclear.
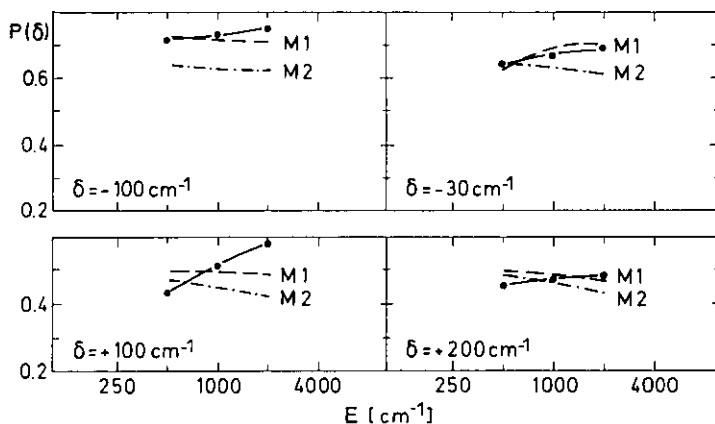

Figure 7. The collisional energy dependence of redistributed polarization in the Sr–He system. The labels are the same as those in figure 2.

An understanding of the behaviour of the polarization seen in the near-blue wing is only obtained after examining the role of the main approximations involved in the model calculations. As discussed, none of the various choices of the decoupling radius leads to a uniformly acceptable reproduction of the polarization curves. The fact that some of them seem to do better must be seen as an artifact in a particular situation, dependent on adjustable parameters. It is important to remember in this context, that the exact orbital rotation angle, as calculated from the CPC solutions of (21) or from the equivalent decoupling radius obtained from them through M3, does not improve the agreement.

However, one cannot blame the discrepancies solely on the approximations inherent in viewing depolarization as coming from the rotation of an orbital after

excitation. Although the CPC solutions of (21) retain more information than merely establishing a rotation angle through (25), their direct application to determine $\alpha^{(2)}$ and $P(\delta)$ does not improve agreement, even though they correspond to a correct description of orbital coupling after excitation, within a classical path description of heavy-particle motion. However, very good agreement occurs between quantal results and the radiatively coupled CPR picture, equations (17) and (18). This shows how the Condon approximation does, indeed, break down near the impact (free atom) regime of the resonance or where antistatic absorption is significant. It is surprising how far this region of invalidity can extend out from line centre.

5. Conclusions

The decoupling radius model seems to give very good qualitative predictions about polarization, and often good quantitative information. Generally, it correctly predicts trends due to changes in detuning, collisional energy, and collision partners. The criteria that have been proposed for the decoupling radius do produce reasonable values, using selection parameters (e.g. β) in a narrow, expected range. There are situations, however, in which these critera do not yield decoupling radii that produce correct polarizations, as in the energy trend for low reduced mass. Though these deficiencies may seem to be correctable with the implementation of simple improvements in the formulae used to determine the decoupling radius, such an approach may be rather dangerous, obscuring the real physics involved. The locking/decoupling radius model must fail in situations in which there are significant contributions from antistatic transitions or the line core.

At least such a procedure should always be compared with the reliable results of classical path method with radiative coupling (CPR), which possesses the capability for analysing the significant and often conflicting influences of impact and antistatic effects. The CPR equations have allowed a systematic study of the approximations involved in the concepts of Condon excitation and of a decoupling radius.

Acknowledgments

References

[1]   Hertel I V, Schmidt H, Bähring A and Meyer E 1985 *Rep. Prog. Phys.* **48** 375
[2]   Greene G H and Zare R N 1982 *Phys. Rev.* A **25** 2031; 1982 *Ann. Rev. Phys. Chem.* **33** 119
[3]   Glass-Maujean M and Beswick J A 1989 *J. Chem. Soc., Trans. Farad. Soc.* II **85** 983
[4]   Burnett K 1985 *Phys. Rep.* **118** 339
[5]   Segal D M and Burnett K 1989 *J. Chem. Soc., Trans. Farad. Soc.* II **85** 925
[6]   Julienne P S and Mies F H 1986 *Phys. Rev.* A **34** 3792
[7]   Kulander K C and Rebentrost F 1984 *J. Chem. Phys.* **80** 5623
[8]   Lewis E L, Slater J M and Harris M 1981 *J. Phys. B: At. Mol. Phys.* **14** L173
      Lewis E L, Harris M, Alford W J, Cooper J and Burnett K 1983 *J. Phys. B: At. Mol. Phys.* **16** 553
[9]   Andersen N 1985 *XII Summer School on Quantum Optics (2–8 September 1985, Frombork, Poland)*

[10] Cooper J 1983 *Spectral Line Shapes* **2** 737
[11] Bieniek R J 1987 *Phys. Rev.* A **35** 3663
[12] Rebentrost F, Best R and Behmenburg W 1987 *J. Phys. B: At. Mol. Phys.* **20** 2627
[13] Behmenburg W, Kroop V and Rebentrost F 1985 *J. Phys. B: At. Mol. Phys.* **18** 2693
[14] Grosser J 1986 *Z. Phys.* **3** 39; 1981 *J. Phys. B: At. Mol. Phys.* **14** 1449
[15] Rebentrost F 1989 *Spectral Line Shapes* **5** 249
[16] Rebentrost F 1989 *J. Chem. Soc., Trans. Farad. Soc.* II **85** 1027
[17] Miller W H 1974 *Adv. Chem. Phys.* **25** 69
[18] Child M S 1974 *Molecular Collision Theory* (New York: Academic)
[19] Kearny W R, Herman P S and Sando K M 1989 *Phys. Rev.* A **40** 7380
[20] Kovalenko L J, Leone S R and Delos J B 1989 *J. Chem. Phys.* **91** 6948
[21] Schatz G C, Kovalenko L J and Leone S R 1989 *J. Chem. Phys.* **91** 6961
[22] Pouilly B and Alexander M H 1990 *Chem. Phys.* **145** 191
[23] Light J C and Szöke A 1978 *Phys. Rev.* A **18** 1363
[24] Delos J B 1981 *Rev. Mod. Phys.* **53** 287
[25] Mies F H, Julienne P S, Band Y B and Singer S J 1986 *J. Phys. B: At. Mol. Phys.* **19** 3249
[26] Szudy J and Baylis W E 1977 *J. Quant. Spectrosc. Radiat. Transfer* **17** 269, 681